Multiphoton Assisted Recombination

E. S. Shuman, R. R. Jones, and T. F. Gallagher
Department of Physics, University of Virginia, Charlottesville, Virginia 22904-4714, USA
(Received 1 September 2008; published 29 December 2008)

We have observed multiphoton assisted recombination in the presence of a 38.8 GHz microwave field. Stimulated emission of up to ten microwave photons results in energy transfer from continuum electrons, enabling recombination. The maximum electron energy loss is far greater than the $2U_p$ predicted by the standard ''simpleman's'' model. The data are well reproduced by both an approximate analytic expression and numerical simulations in which the combined Coulomb and radiation fields are taken into account.

DOI: 10.1103/PhysRevLett.101.263001 PACS numbers: 32.80.Rm, 32.80.Wr

Two decades ago the ''simpleman's'' model (SM) was introduced to explain the range of electron energies produced during the above-threshold ionization of atoms in intense laser fields [1–3]. Based on classical mechanics, the SM neglects the binding potential of the parent ion, obtaining an analytic expression for the energy transfer to or from a free electron which is instantaneously inserted into an oscillating electric field. Beyond above-threshold ionization, the simpleman's framework accurately predicts the high-energy cutoff observed in high-harmonic generation [4] as well as the maximum energy exchange between a high-energy continuum electron and a relatively weak laser field [5]. The latter of these has been exploited to determine the duration of ultrashort extreme ultraviolet and x-ray pulses [6–8], characterize the duration and spectral phase of attosecond pulses [9–11], reconstruct the electric field in a few-cycle laser pulse [12], and probe attosecond electron wave packet dynamics [13,14].

Here we consider the situation in which the oscillating field extracts sufficient energy from a continuum electron to recombine it with its parent ion. Specifically, we photoexcite low energy continuum electrons from Ba in the presence of a 38.8 GHz microwave pulse. At the end of the pulse some electrons have been recombined with their parent ions. The maximum recombination energy transfer greatly exceeds that predicted by the SM. However, it is well reproduced by a classical model in which the Coulomb and radiation fields are taken into account.

Our results are also relevant in the context of electron-ion recombination [15], a topic with applicability in fields from high temperature plasmas to the formation of antihydrogen [16]. Formally, the process we study is stimulated radiative recombination [17]. However, as with other nonresonant multiphoton phenomena, the germane physics is most easily understood in terms of momentum transfer between a classical field and a continuum electron. In fact, the process is analogous to electron-ion recombination stimulated by isolated half-cycle pulses [18].

We excite electrons with well-defined energies $|E_0| < 15\ \mathrm{cm}^{-1}$ relative to the ionization threshold, in the presence of a pulsed 38.8 GHz microwave field. A novel scheme, based on radiative stabilization of autoionizing Rydberg states, facilitates pulsed field-ionization detection of only those atoms with electrons bound by $<1\ \mathrm{cm}^{-1}$ following the microwave pulse [19,20].

Ba atoms in a thermal beam pass through a Fabry-Pérot microwave cavity perpendicular to its axis. The atoms are excited at the center of the cavity by three pulsed dye lasers. The first two lasers counterpropagate with the atomic beam and are fixed in frequency to drive the transitions $6s^2 \rightarrow 6s6p \rightarrow 6s11d$. The third beam propagates along the horizontal cavity axis and further excites the $6s11d$ Rydberg atoms to the broad, $6p_{3/2}11d$ autoionizing resonance. The third laser frequency can be tuned to vary the total excitation energy E_0, which we define relative to the Ba^+ $6p_{1/2}$ ionization threshold as shown in Fig. 1. Parallel plates are positioned above and below the cavity to enable field ionization of highly excited $6s_{1/2}nd$ Rydberg atoms produced via recombination. The upper plate has a 1 cm diameter hole through which the resulting electrons pass en route to a microchannel plate detector.

The Fabry-Pérot cavity consists of two brass mirrors of 9.734 cm radius of curvature with a 4.65 cm on axis separation. It is operated in the TE^{09} mode, which has a frequency 38.8 GHz, and a Q of 780. The microwave source is an Agilent 83622D frequency synthesizer operating at 19.4 GHz followed by a Hewlett Packard (HP) 83554A doubler and Phase 1 SP40-2529 amplifier which produces up to 500 mW of power at $\omega/2\pi = 38.8$ GHz. We use a 20 dB coupler to monitor the power with a HP R422A crystal detector, which has been calibrated against an Agilent 432A thermal power meter. We can determine the microwave field amplitude in the cavity, F_0, with an uncertainty of 20%.

The three sequential 5 ns laser pulses are incident on the atoms while the microwave field is present in the cavity. The microwave source is switched off 5 ns after the last laser pulse, and the field in the cavity decays with a 64 ns time constant. An 800 V pulse with a 50 ns rise time is applied to the lower field plate 1 μs after the laser pulses. It produces a peak field of 160 V/cm, which ionizes bound $6sn\ell$ atoms with $n > 38$. The field ionization signal is recorded as a function of the third laser frequency.

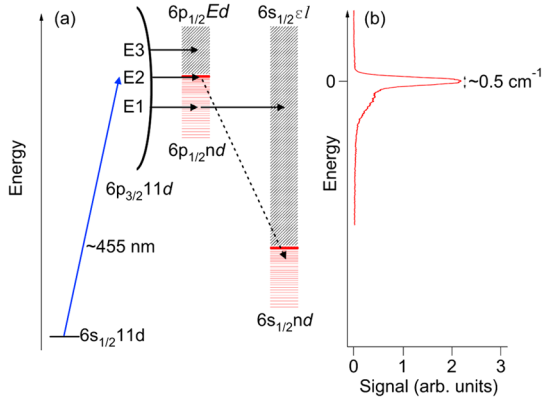

FIG. 1 (color online). (a) Diagram of essential energy levels and schematic of radiative stabilization of highly excited $6p_{1/2}nd$ autoionizing states in the absence of the microwave field. At excitation energies above the $6p_{1/2}$ limit ($E_0 = E3$), ionization is immediate. For a small range of excitation energies ($E_0 = E2$) just below the $6p_{1/2}$ limit the atoms are stabilized by radiative decay. For more tightly bound states ($E_0 = E1$) the atoms autoionize. Autoionization into the degenerate $5d_j\epsilon'\ell$ channels (not shown) plays no essential role in the radiative stabilization process. (b) Measured field ionization signal versus excitation energy relative to the Ba^+ $6p_{1/2}$ limit.

As shown schematically in Fig. 1(a), Ba atoms are photoexcited to a broad $6p_{3/2}11d$ autoionizing resonance which straddles the Ba^+ $6p_{1/2}$ ionization threshold. Atoms in the $6p_{3/2}11d$ state quickly decay (in $\approx$1 ps) into the degenerate $6p_{1/2}Ed$, $5d_j\epsilon\ell$, or $6s_{1/2}\epsilon'\ell'$ configurations. Electrons with energies $\epsilon \approx 1.9$ eV and $\epsilon' \approx 2.5$ eV in the respective $5d_j$ and $6s_{1/2}$ continua rapidly leave the vicinity of the Ba^+ ion regardless of the microwave field amplitude. The recombination measurements are sensitive only to population transferred to the $6p_{1/2}Ed$ configuration.

Once in the $6p_{1/2}Ed$ channel, the fate of the atom depends on the Rydberg electron energy E. Consider the situation with no microwaves present. If $E = E_0 > 0$, $6p_{1/2}Ed$ continuum states are populated, resulting in immediate ionization. If $E = E_0 < 0$ ($= -1/2n^2$), $6p_{1/2}nd$ bound states are created. These typically decay via autoionization rather than spontaneous emission. However, for very highly excited states ($n > 300$) the n-independent spontaneous emission rate of the Ba^+ $6p_{1/2}$ electron exceeds the $6p_{1/2}nd$ autoionization rate which scales as n^{-3} [20]. Therefore, over a small energy range, $-0.5\ \mathrm{cm}^{-1} < E_0 < 0$, most of the $6p_{1/2}nd$ population decays into stable $6s_{1/2}nd$ Rydberg states [19]. As shown in Fig. 1(b) these can then be detected by pulsed field ionization [20]. The third laser frequency determines the initial energy $E = E_0$, but in the presence of the microwave field electron energy is not conserved following the laser excitation. The absorption (emission) of microwave photons can result in a discrete increase (decrease) in E. Regardless of the excitation energy, if a Rydberg electron has energy $-0.5\ \mathrm{cm}^{-1} < E \simeq 0$ after the microwave pulse, then the atom is radiatively stabilized and will be detected via pulsed field ionization. The difference between a detected electron's initial energy, $E = E_0$, and final energy, $E \simeq 0$, gives the energy transfer in the microwave field.

Figure 2 shows the field ionization signal versus excitation energy for different microwave field strengths. As the field is increased, additional peaks separated by the microwave photon energy appear on either side of the zero-field stabilization peak. For excitation energies $E_0 < (>) 0$, this structure is the result of stimulated absorption (emission) of microwave photons to final states with $E \simeq 0$. To our knowledge, the peaks appearing at $E_0 > 0$ represent the first observation of multiphoton assisted recombination in a microwave field, and their energy extent is the primary focus of this Letter. We stress that the additional peaks are not subsidiaries of the zero-field, radiative stabilization signal. Instead, at each excitation energy, the microwave field generates sidebands in the probability density for the $6p_{1/2}$ channel. When one of these sidebands has energy $E \simeq 0$, a fraction of the atoms are stabilized and a peak in the field ionization signal is produced. The energy extent ΔE_+ of the sidebands observed for $E_0 < 0$ reflects the maximum energy transfer to initially bound electrons. The extent ΔE_- of the sidebands for $E_0 > 0$ reveals the maximum energy extraction from continuum electrons.

The data in Fig. 2 show that $\Delta E_{+,-}$ are proportional to microwave field strength and much larger than the ponderomotive shift, $U_p = F_0^2/4\omega^2$ (a.u.). U_p is only 0.15 cm^{-1} at the largest field strength studied.

To predict the energy extent of the recombination sidebands, we consider an electron with energy $E_0 > 0$, launched at time $t = 0$ from the origin of a Coulomb

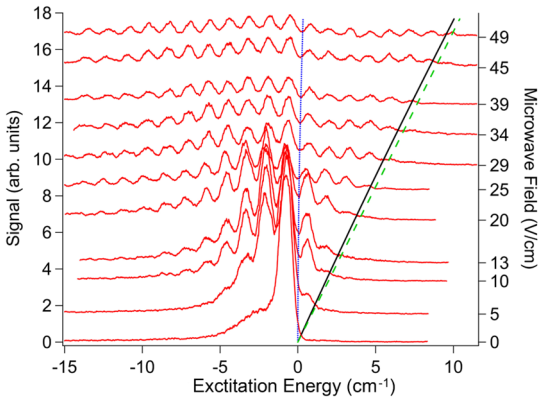

FIG. 2 (color online). Field ionization signal as a function of excitation energy E_0 for different microwave fields, $0 \le F_0 \le 49$ V/cm. The energy scale is relative to the Ba^+ $6p_{1/2}$ limit. The baseline of each trace is displaced by the microwave field amplitude, according to the scale on the right-hand axis. The blue dotted line and green dashed line show the maximum recombination energy ΔE_- predicted by Eqs. (3) and (4), respectively. The black solid line shows the maximum recombination energy found in the CTMC simulation.

potential in the presence of a linearly polarized, oscillating electric field, $F_0(t)\cos\omega(t-t_0)$ (see Fig. 3). The field amplitude $F_0(t)$ is very slowly varying compared to the oscillation period $T = 2\pi/\omega$ and has a peak value F_0. Electrons detected with final energy $E \simeq 0$ have lost an amount of energy, E_0, in the field. We wish to determine, as a function of F_0, the maximum value $E_0 = \Delta E_-$ for which recombination can occur.

During the time interval $0 \le t \le t_f$, the work done on a classical electron by the field $F(t)$ is

$$W = -\int_0^{t_f} \vec{F(t)} \cdot \vec{v(t)} dt, \tag{1}$$

where $\vec{v(t)}$ is the electron's velocity and, unless otherwise noted, atomic units are used. Maximum energy transfer is achieved for motion in one dimension. This is a reasonable approximation for $6p_{1/2}Ed$ continuum electrons launched parallel to the field axis. However, even in one dimension, v is a nontrivial function of time, and W must be computed numerically for different values of $F_0(t)$, E_0, ω, and t_0. The SM avoids this complexity by neglecting the Coulomb potential and is the standard approach for treating continuum electron dynamics in oscillating fields.

In the SM, $v(t)$ is obtained from the initial velocity, $v_0 = \sqrt{2E_0}$, by integrating the acceleration due to the lone force, $F(t)$. Technically, the use of Eq. (1) requires knowledge of the temporal field envelope $F_0(t)$. However, in any time interval, $0 \le t \le t_f$, the momentum transferred to a *free* electron in a spatially uniform electric field is proportional to the change in the vector potential, $A(t_f) - A(0)$ [21]. Moreover, in the slowly varying envelope approximation, the vector potential of a nominally monochromatic field pulse oscillates symmetrically about its postpulse value, $A(t = \infty)$, and is equal to $A(t = \infty)$ when the field magnitude is maximum, twice during each field cycle. Stated differently, if the field turns off slowly, the energy gain or loss during each *complete* half-cycle is precisely canceled by that during the next half-cycle. Therefore, the net momentum (and energy) change during the entire microwave pulse is equal to that transferred in the interval $0 \le t \le t_0$. Accordingly, we set $t_f = t_0$ in Eq. (1) to obtain the SM result [22]

$$W = 2U_p \sin^2\omega t_0 - \sqrt{8U_p E_0}\sin\omega t_0. \tag{2}$$

From Eq. (2) it is straightforward to show that for a given F_0, the maximum E_0 for which recombination can occur is

$$\Delta E_- = 2U_p = \frac{F_0^2}{2\omega^2}. \tag{3}$$

This maximum energy extraction requires electron launch at a zero of the field, i.e., $t_0 = T/4$.

The SM [Eq. (3)] fails to explain our measurements (see Fig. 2). First, the data in Fig. 2 exhibit a linear dependence of ΔE_- on F_0 while Eq. (3) predicts a quadratic dependence. Second, the magnitude of the prediction is too small by over 2 orders of magnitude for the lowest field studied and by more than a factor of 30 at the highest field.

The shortcoming of the SM is its neglect of the atomic potential [21,23]. The electron's velocity in Eq. (1) is determined by its kinetic energy K, not E_0. In the SM, $K = E_0$, but in our experiment, and in a Coulomb potential generally, it is not. As illustrated in Fig. 3, for $E_0 \ll 1$ a.u., $K \gg E_0$ at small distances r from the ion. Moreover, slight changes in E have a negligible effect on K near the nucleus, where $K \simeq 1/r$ and $v(t) = v_0(t) \simeq \sqrt{2/r(t)}$. The fact that this velocity expression may not be accurate at large r is not important when computing the work done by the field [see Eq. (1)]. The dominant contribution to W comes from early times where the electron's speed, $v(t) = \sqrt{2/r(t)} = (\frac{4}{3t})^{1/3}$, is greatest and independent of $F(t)$ and E_0.

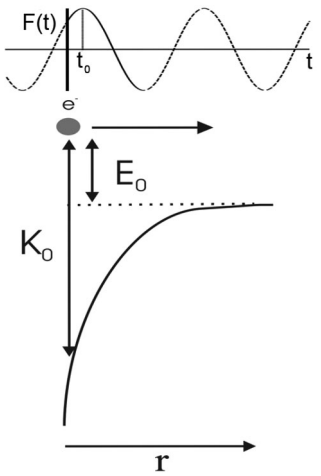

FIG. 3. Illustration of the launch of a classical electron with initial energy E_0 from the origin of a Coulomb potential at $t = 0$. The first maximum in the applied oscillating electric field $F(t)$ (dashed line) occurs at a time $t = t_0$. The relevant energy transfer from the field to the electron occurs in less than one cycle of the field $0 \le t \le t_f$ [solid line portion of $F(t)$] due to the rapid decrease in K with increasing r.

Unlike the free electron case, the work done by the field in consecutive half-cycles does not precisely cancel. However, given the rapid decrease in the electron's time-averaged velocity with increasing r, we find that the net contribution to the energy transfer is minimal after one additional half-cycle. Therefore, we truncate the integral in Eq. (1) at $t_f = t_0 + T/2$ (see Fig. 3). This is equivalent to assuming that changes in the Coulomb potential are negligible during subsequent half-cycles. We then evaluate Eq. (1) analytically by approximating the first two half-cycles of the sinusoidal field as a sum of two parabolas with identical widths and equal, but opposite, amplitudes [24]. The full duration, $T_p = 3T/2\pi$, of each parabolic half-cycle is scaled so that the impulse it delivers is equal to that provided by one half-cycle of a sinusoid with the same amplitude. We obtain a maximum energy transfer

$$\Delta E_- \simeq 3/2 F_0 \omega^{-2/3} \tag{4}$$

when $t_0 \simeq T/6$. Equation (4) predicts a linear dependence of ΔE_- on F_0, and as shown in Fig. 2, is in excellent agreement with the measured extent of the recombination. The predicted optimum launch time, $t_0 \simeq T/6$, is a compromise between two competing effects, maximizing the interval during which F and v have the same sign ($t_0 \simeq T/4$), and simultaneously maximizing F and v ($t_0 = 0$).

It is prudent to assess the validity of the approximations made in formulating Eq. (4). First, using the field-free electron velocity results in negligible errors as long as $\Delta E_- \gg U_p$. Second, the approximation $E_0 \approx 0$ can be improved by computing the energy transfer associated with the next higher order term in the series expansion, $v_0 \simeq \sqrt{2/r}(1 + E_0 r/2)$. This gives $\Delta E_- \simeq 3/2 F_0 \omega^{-2/3}(1 + 0.2 E_0 \omega^{-2/3})$, which differs from Eq. (4) by 3% for the highest energies used in our experiments. Equation (4) should also be valid for determining the maximum energy transfer ΔE to an electron in a *laser-dressed* continuum provided $E_0 < \omega^{2/3}$ and $\Delta E \gg U_p$.

Classical trajectory Monte Carlo (CTMC) simulations of the experiment support the interpretation presented above. In our calculation, an ensemble of approximately 1000 electrons, with identical total energy $E_0 > 0$ and total angular momentum $L = 2$, are launched from the inner turning point of a hyperbolic orbit in the presence of a Coulomb field and 38.8 GHz microwave pulse. The electron launch times within the field cycle and the orientations of the orbits relative to the microwave polarization are randomly distributed. Newton's equations of motion are integrated for each electron for the remainder of the microwave pulse. The final energy distribution for the ensemble is recorded as a function of initial energy E_0 and microwave field strength. Values for ΔE_- extracted from these distributions are plotted in Fig. 2. The agreement between the data, the prediction of Eq. (4), and the simulation results is excellent. In addition, the simulation reproduces the predicted second-order corrections to both ΔE_- and the phase at which the maximum energy transfer occurs (see preceding paragraph) for values of E_0 larger than those explored in the experiment.

Our model predicts an equivalent, maximum energy gain ΔE_+ for electrons with initial velocities antiparallel to the field. Indeed, this is the source of the negative energy sidebands in the field ionization spectrum although the dynamics are more complex. At all but the very lowest binding energies, bound electrons periodically pass the nucleus and have multiple opportunities to gain (and lose) energy in the field. Therefore, we attribute the smaller extent and amplitude of the peaks at $E_0 > 0$ to the fact that continuum electrons have only one chance to interact with the combined microwave-Coulomb potential as they move out from the core.

In conclusion, we report the first measurements of multiphoton assisted recombination in a microwave field. The data indicate that recombination is possible at energies far in excess of those predicted by the SM. The measurements underscore the fact that at low electron energies and weak to intermediate dressing fields the Coulomb potential plays a critical role in driven electron dynamics. The data are well reproduced by an approximate model and CTMC simulations in which both the Coulomb and dressing potentials are taken into account. The expressions we derive provide an alternative to the SM for determining energy transfer to or from electrons in a regime that is relevant to some recent laser experiments as well. It would be most interesting to see a quantum mechanical treatment of this problem as well as experimental verification of the phase dependence of the energy transfer.

This work has been supported by the U.S. Department of Energy, Office of Basic Energy Sciences.

[1] H. B. van Linden van den Heuvell and H. G. Muller, *Multiphoton Processes*, edited by S. J. Smith and P. L. Knight (Cambridge University Press, Cambridge, England, 1988).
[2] T. F. Gallagher, Phys. Rev. Lett. **61**, 2304 (1988).
[3] P. B. Corkum, N. H. Burnett, and F. Brunel, Phys. Rev. Lett. **62**, 1259 (1989).
[4] J. L. Krause, K. J. Schafer, and K. C. Kulander, Phys. Rev. Lett. **68**, 3535 (1992); K. J. Schafer *et al.*, *ibid.* **70**, 1599 (1993).
[5] J. M. Schins *et al.*, Phys. Rev. Lett. **73**, 2180 (1994).
[6] T. E. Glover *et al.*, Phys. Rev. Lett. **76**, 2468 (1996).
[7] M. Hentschel *et al.*, Nature (London) **414**, 509 (2001).
[8] L. Miaja-Avila *et al.*, Phys. Rev. Lett. **97**, 113604 (2006).
[9] P. M. Paul *et al.*, Science **292**, 1689 (2001).
[10] R. Lopez-Martens *et al.*, Phys. Rev. Lett. **94**, 033001 (2005).
[11] G. Sansone *et al.*, Science **314**, 443 (2006).
[12] E. Goulielmakis *et al.*, Science **305**, 1267 (2004).
[13] P. Johnsson *et al.*, Phys. Rev. Lett. **95**, 013001 (2005).
[14] J. Mauritsson *et al.*, Phys. Rev. Lett. **100**, 073003 (2008).
[15] R. Flannery, *Atomic, Molecular, and Optical Physics Handbook* (AIP, Woodbury, NY, 1996).
[16] G. Gabrielse *et al.*, Phys. Rev. Lett. **89**, 233401 (2002).
[17] U. Schramm *et al.*, Phys. Rev. Lett. **67**, 22 (1991); F. B. Yousif *et al.*, *ibid.* **67**, 26 (1991).
[18] T. J. Bensky, M. B. Campbell, and R. R. Jones, Phys. Rev. Lett. **81**, 3112 (1998).
[19] J. G. Story, B. J. Lyons, and T. F. Gallagher, Phys. Rev. A **51**, 2156 (1995).
[20] T. F. Gallagher, *Rydberg Atoms* (Cambridge University Press, Cambridge, England, 1994), 1st ed.
[21] U. Saalmann and J. M. Rost, Phys. Rev. Lett. **100**, 133006 (2008).
[22] L. F. DiMauro and P. Agostini, Adv. At. Mol. Opt. Phys. **35**, 79 (1995).
[23] H. S. Nguyen, A. D. Bandrauk, and C. A. Ullrich, Phys. Rev. A **69**, 063415 (2004).
[24] R. R. Jones, D. You, and P. H. Bucksbaum, Phys. Rev. Lett. **70**, 1236 (1993).